Investigation of the electric field distribution in the human brain based on MRI and EEG data

Yu.V. Kistenev[a,b], A.V. Borisov[a,b], A.I. Knyazkova[a], A.V. Shapovalov[a], E.E. Ilyasova[a,b], E.A. Sandykova[a,b]

[a]Tomsk State University, 36 Lenina ave., Tomsk, Russian Federation

[b]Siberian State Medical University, 2 Moskovskiy tract, Tomsk, Russian Federation

ABSTRACT

This work is devoted to the development of the approach to restoration of the spatial-temporal distribution of electric field in the human brain. This field was estimated from the model derived from the Maxwell's equations with boundary conditions corresponding to electric potentials at the EEG electrodes, which are located on the surface of the head according to the standard "10-20" scheme. The MRI data were used for calculation of the spatial distribution of the electrical conductivity of biotissues in the human brain. The study of the electric field distribution using our approach was carried out for the healthy child and the child with autism. The research was carried out using the equipment of the Tomsk Regional Common Use Center of Tomsk State University.

Keywords: electric field spatial distribution of the human brain, EEG, MRI, Maxwell's equations, autism

1 INTRODUCTION

A lot of efforts is devoted to the investigation of the disorders of human brain. Classification of EEG signals plays an important role in the diagnosis and treatment of brain diseases. A new approach for detection of epilepsy using EEG is based on the nonlinear nature of EEG data.[1] Many studies are devoted to the study of EEG coherence in the state of rest for various addictions. Neural connectivity and the level of phasic synchronization between neural populations in patients with Internet gaming disorder (IGD), patients with alcohol use disorder (AUD), and healthy controls (HCs) using resting-state EEG coherence analyses was analyzed.[2] The results show that IGD and AUD are associated with different neuropathological patterns of brain connectivity and more strong neuronal synchronization of the frequency bands can be neuropathological characteristics of IGD. Peculiarities in the power and coherence of the EEG in different frequency ranges in the hypnotic state for smokers were obtained.[3] It was shown that EEG coherence increases in the delta and theta bands and decreases in the alpha and beta bands. EEG data could be utilized as objective markers to screen the AUD patients and healthy controls on a base of integration of the theta, beta, and gamma power and inter-hemispheric coherence.[4] To classify EEG signals in different mental states, an approach based on an artificial neural network is used.[5] The experimental results show that the proposed method is superior to other classifiers.

Alcin O. F. and co-authors used various methods for processing EEG signals, such as the frequency-time representation of the gray coincidence descriptors (GLCM) and Fisher Vector (FV) for the automatic classification of EEG signals.[6] The detection of moving images by classification of EEG signals is also considered.[7] The experimental results show that the proposed method based on the analysis of independent components has a high accuracy of classification.

The magnetic resonance imaging (MRI) is used in useful for diagnostics in various fields of medicine, such as oncology, neurology, gynecology and others. The variations of MRI parameters under a disorder of the central nervous system were also studied.[8]

Detailed morphometric analysis of the neonatal brain is useful to characterize the development of the brain and to determine neurovascular biomarkers associated with impaired brain growth. The algorithm for constructing an unbiased four-dimensional atlas of the developing fetal brain was developed, and also the use of such atlas for automatic segmentation of the fetal brain MRT.[9]

International Conference on Atomic and Molecular Pulsed Lasers XIII, edited by Victor F. Tarasenko, Andrey M. Kabanov, Proc. of SPIE Vol. 10614, 106141P
 · doi: 10.1117/12.2303464

The method of automatic segmentation of MRI of newborns is used to detect cortical grooves and to provide detailed delineation of cortical tape.[10] Detailed segments are used to construct a 4-dimensional space-time structural atlas of the brain. Gholipour A. and co-authors developed an algorithm for constructing an unshifted four-dimensional atlas of the developing fetal brain and evaluated the use of this atlas and additional individual fetal brain MRI-atlases for automatic segmentation of the fetal brain MRI.[11] This atlas is available online as a reference for anatomy, as well as for registration and segmentation.

It should be noted that metal implants can disrupt MRI images, which can cause interpretation errors. The Au-35Pt alloy magnetic susceptibility is very close to the susceptibility of living tissue and does not cause artifacts during MRI.[12] This alloy is useful to make intracranial electrodes, coils embolizing brain aneurysm, markers for MRI, and etc.

The simultaneous registration of EEG and MRI can help to overcome the space-time limitations of each method separately and is more effective tool for studying human brain. The hybrid neuroimaging was used to study the effect of strong magnetic fields on the activity of the human brain, exceeding the current recommendations of the International Commission on Non-Ionizing Radiation Protection (ICNIRP) and the Institute of Electrical and Electronics Engineers (IEEE).[13] The combined EEG and MRI was carried out to characterize the possible spatial-temporal patterns of brain activity with high resolution of magnetic flux density.[16] The results of this study confirmed the absence of specific acute effects on the activity of the human brain under magnetic field action up to 7.6 mT, which is consistent with the limitations by both ICNIRP and IEEE magnetic field levels. [14,15]

The simultaneous usage of EEG and MRI for the study of functional and microstructural correlations of glutamate were analyzed. The absolute concentration of glutamate in the gray matter was calculated and these values were checked for correlation with the metric of the stationary image of the diffusion tensor, functional MRI and electric EEG sources. Real-time analysis with simultaneous registration of EEG and MRI is necessary in the study of neurofeedback and in the effective monitoring of brain activity. However, the artifacts of the ballistic histogram caused by movements associated with the heart rhythm in the MRI scanner strongly contaminate EEG signals and interfere with reliable real-time analysis. To solve this problem, the authors use the method of optimal basic sets in real time for removal of the ballistic histogram artifacts.[17]

Thus, simultaneous usage of EEG and MRI for the study of human brain activity is promising approach. This work is devoted to the restoration of the electric field spatial distribution of the human brain using both the MRI and EEG data.

2 MATERIALS AND METHODS

We used experimental EEG and MRI data were obtained for a healthy child aged 6 years and a child with autism at the age of 8 years. The children watched a video when EEG data were recorded. The experimental data were collected by EEG and MRI obtained independently by standard way as follows.

The experimental EEG data were obtained using a standard digital 16-channel electroencephalograph with EEG18 V5.0.3 software. The arrangement of electrodes were according to the standard “10-20” scheme (Fig. 1).

The EEG was recorded by measuring the potential difference between the reference electrode located outside of the head and the extracranial electrodes which were located on the surface of the head. The EEG records contained electric oscillations within the 0.8-30 Hz frequency range and 30 mm /s scan rate. The sampling rate was 100 Hz/s, sampling discretization was 12 bits, the input resistance was more than 10 MΩ. Digital recursive filtering and Fourier transform was used for the EEG analysis in specific frequency ranges.

MRI was recorded by high-precision 2-Tesla MRI-tomograph (Siemens) in Tomsk Diagnostic Center licensed for this type of activity.

Mathematical approach includes the following equations.
Standard continuity equation:

$$\nabla \boldsymbol{j} + \frac{\partial \rho}{\partial t} = 0 , \quad (1)$$

here $\boldsymbol{j}$ is the current density, $\partial\rho/\partial t$ is the time derivative of the charge density.

The Ohm's law:

$$\boldsymbol{j} = \sigma \boldsymbol{E} \ , \tag{2}$$

here σ is the conductivity, $\boldsymbol{E}$ is the electric field vector.

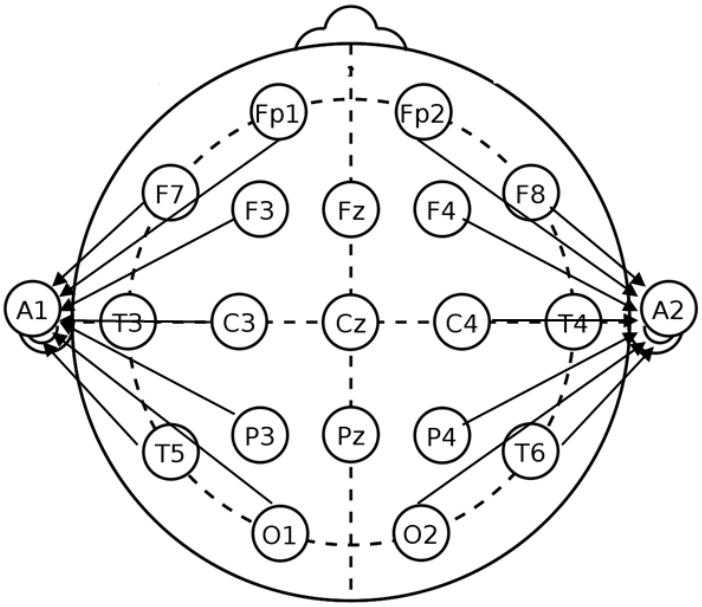

Channel list	
1	Fp1–A1
2	Fp2–A2
3	F3–A1
4	F4–A2
5	C3–A1
6	C4–A2
7	P3–A1
8	P4–A2
9	O1–A1
10	O2–A2
11	F7–A1
12	F8–A2
13	T3–A1
14	T4–A2
15	T5–A1
16	T6–A2

Figure 1. Electrode locations of International 10-20 system for EEG recording

To solve equation (1) it is necessary to know the boundary conditions and conductivity value of brain tissues at each point. The boundary conditions for electric field can be derived from EEG experimental data.
To estimate the spatial distribution conductivity we used the following approach. The base was the Maxwell equation for magnetic field:

$$\nabla \times \boldsymbol{H} = \boldsymbol{j} + \frac{\partial \boldsymbol{D}}{\partial t} \ , \tag{3}$$

where $\boldsymbol{H}$ is the vector of the magnetic field, $\boldsymbol{D}$ is the electric induction. The electrical properties of the human brain tissues vary slowly with time (the useful frequencies in bio-electromagnetic phenomena are usually below 1 kHz), therefore the time dependence in (3) can be neglected. Thus, let $\partial \boldsymbol{D}/\partial t = 0$ when using MRI data.
Substituting (2) into equation (3), we obtain

$$\nabla \times \boldsymbol{H} = \sigma \boldsymbol{E}. \tag{4}$$

Equation (4) can be used to find the conductivity, if the distribution of the electric and magnetic fields in the brain are known. The distribution of magnetic field was described by MRI experimental data. The electric field vector on the surface of the head was described by EEG experimental data as mentioned above. Thus, we have a self-consistent system of equations.

3 RESULTS

The above mentioned system of equations was solved using layer-by-layer calculation by finite element numerical method. As a result, the spatial-temporal dependences of the $\boldsymbol{E}$ (x, y, z, t) and $\boldsymbol{j}$ (x, y, z, t) and the average energy of the electric field W(t) in the brain were calculated.
Figure 2 shows the spatial distribution of the square of the electric field value in the brain, figure 3 shows the dependence of the energy of the electric field on time for the healthy child and the child with autism.

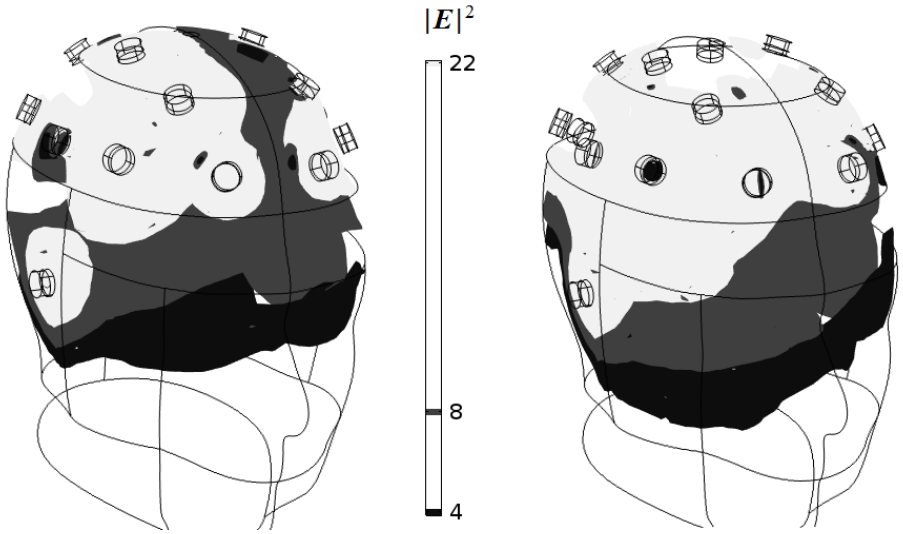

Figure 2. The spatial distribution of the the square of the electric field value the healthy child (A) and the child with autism (B).

According to the Figure 2 isosurfaces of the electric field value for the child with autism in common directed in the horizontal place.

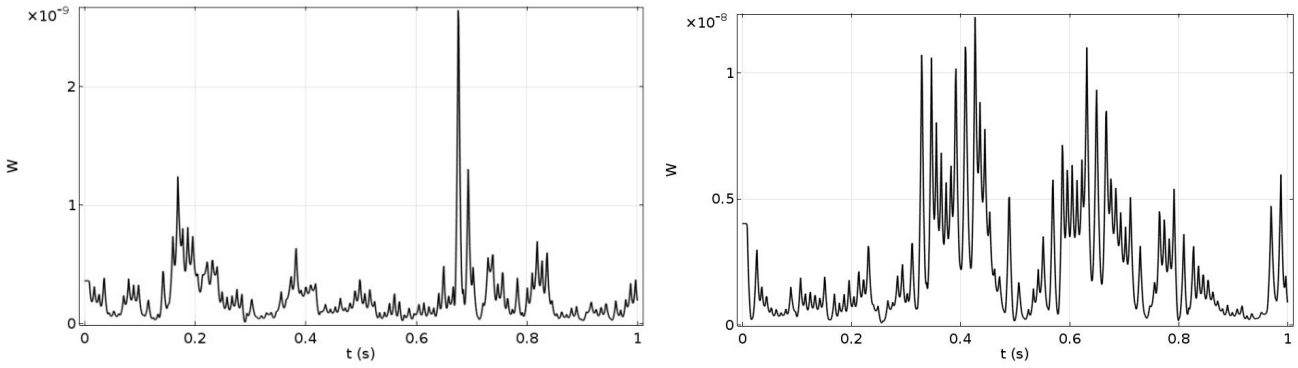

Figure 3. The dependence of the energy of the electric field on time for a healthy child (left image) and a child diagnosed with autism (right image).

According to the Figure 3 the time dependence of the square of the electric field value in the brain for the healthy child has sharp peaks at t = 0.68s, which are not observed for the child with autism. The following frequency bands are considered: delta (0-4 Hz), theta (4-8 Hz), alpha (8-12 Hz), beta (12-30 Hz) and gamma (30- 100 Hz). In the study of autism spectrum disorders, theta and alpha ranges are the most informative.[18, 19]

Figure 4 shows the electric field values in the theta and alpha frequency ranges. Evidently, that in the alpha range the electric field value for the child with autism is significantly weaker than that for the healthy child, which agrees with the results obtained using standard EEG method.[18, 19]

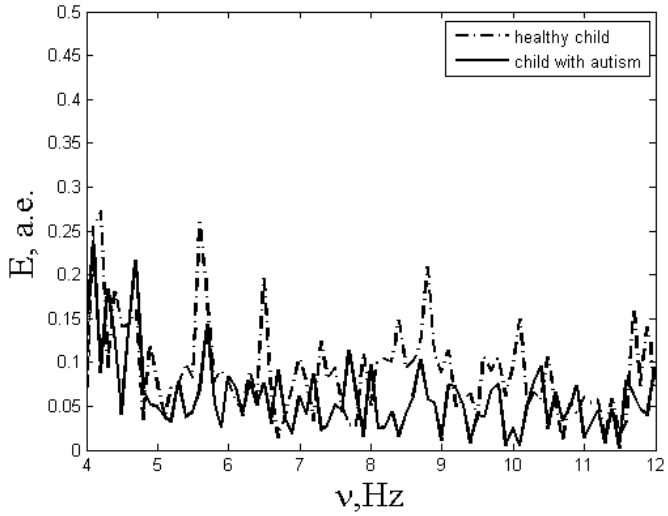

Figure 4. Spectral dependence of the electric field value in the theta and alpha frequency ranges for a healthy child and a child with autism.

4 CONCLUSION

This presented approach allows to restore the spatial and temporal distribution of electric field in the human brain using the MRI and EEG experimental data. The time dependences of the spatial distribution of electric field in the human brain were obtained. The obtained results in are in qualitative agreement with the standard approaches.

The approach and its analogues are characterized by the laboriousness of implementation and large computing resources.[20,21] However, these methods are promising for obtaining new data for different psychological diseases, including autism disorder.

References

[1] Martinez-del-Rincon, J., Santofimia, M. J., del Toro, X., Barba, J., Romero, F., Navas, P., & Lopez, J. C., "Non-linear classifiers applied to EEG analysis for epilepsy seizure detection," Expert Systems with Applications, 86, 99-112 (2017). doi:10.1016/j.eswa.2017.05.052

[2] Park, S. M., Lee, J. Y., Kim, Y. J., Lee, J., Jung, H. Y., Sohn, B. K., Choi, J., "Neural connectivity in internet gaming disorder and alcohol use disorder: A resting-state EEG coherence study," Scientific Reports, vol. 7, no. 1 (2017). doi:10.1038/s41598-017-01419-7

[3] Li, X., Ma, R., Liangjun, P., Lv, W., Xie, Y., Chen, Y., Xiaochu, Z., "Delta coherence in resting-state EEG predicts the reduction in cigarette craving after hypnotic aversion suggestions," Scientific Reports, vol. 7, no. 1 (2017). doi:10.1038/s41598-017-01373-4

[4] Mumtaz, W., Vuong, P. L., Xia, L., Malik, A. S., & Rashid, R. B. A., "An EEG-based machine learning method to screen alcohol use disorder," Cognitive Neurodynamics, 11(2), 161-171 (2017). doi:10.1007/s11571-016-9416-y

[5] Anh, N. T. H., Hoang, T. H., Dung, D. T., Thang, V. T., & Bui, T. T. Q., "An artificial neural network approach for electroencephalographic signal classification towards brain-computer interface implementation," Paper presented at the 2016 IEEE RIVF International Conference on Computing and Communication Technologies: Research, Innovation, and Vision for the Future, RIVF 2016 - Proceedings, 205-210 (2016). doi:10.1109/RIVF.2016.7800295

[6] Alçin, Ö. F., Siuly, S., Bajaj, V., Guo, Y., Şengu¨r, A., & Zhang, Y.," Multi-category EEG signal classification developing time-frequency texture features based fisher vector encoding method," Neurocomputing, 218, 251-258 (2016). doi:10.1016/j.neucom.2016.08.050

[7] Olivier, T. E., Du, S., & Van Wyk, B. J., "Independent components for EEG signal classification," Paper presented at the ACM International Conference Proceeding Series (2016). doi:10.1145/3028842.3028875
[8] Kim, S., Park, E. Y., Park, B., Hyun, J., Park, N. Y., Joung, A., Kim, H. J. "Multimodal magnetic resonance imaging in relation to cognitive impairment in neuromyelitis optica spectrum disorder," Scientific Reports, 7(1) (2017). doi:10.1038/s41598-017-08889-9
[9] Gholipour, A., Rollins, C. K., Velasco-Annis, C., Ouaalam, A., Akhondi-Asl, A., Afacan, O., Warfield, S. K., "A normative spatiotemporal MRI atlas of the fetal brain for automatic segmentation and analysis of early brain growth," Scientific Reports, 7, n.1 (2017). doi:10.1038/s41598-017-00525-w
[10] Makropoulos, A., Aljabar, P., Wright, R., Hüning, B., Merchant, N., Arichi, T., Rueckert, D., "Regional growth and atlasing of the developing human brain," NeuroImage, 125, 456-478 (2016). doi:10.1016/j.neuroimage.2015.10.047
[11] Gholipour, A., Rollins, C. K., Velasco-Annis, C., Ouaalam, A., Akhondi-Asl, A., Afacan, O., Warfield, S. K., "A normative spatiotemporal MRI atlas of the fetal brain for automatic segmentation and analysis of early brain growth," Scientific Reports, 7(1) (2017). doi:10.1038/s41598-017-00525-w
[12] Kodama, T., Nakai, R., Goto, K., Shima, K., & Iwata, H., "Preparation of an au-pt alloy free from artifacts in magnetic resonance imaging," Magnetic Resonance Imaging, 44, 38-45 (2017). doi:10.1016/j.mri.2017.07.006
[13] Modolo, J., A. W. Thomas, and A. Legros., "Human Exposure to Power Frequency Magnetic Fields Up to 7.6 mT: An Integrated EEG/fMRI Study," Bioelectromagnetics, 38, no. 6, 425-435 (2017). doi:10.1002/bem.22064
[14] Wolters Kluwer Health, "Guidelines for limiting exposure to time-varying electric and magnetic fields (1 Hz to 100 kHz)," Health Physics: The Radiation Safety Journal, 99, 818–836 (2010).
[15] IEEE C95.6-2002, "IEEE Standard for safety levels with respect to human exposure to electromagnetic fields, 0–3 kHz," The Institute of Electrical and Electronics Engineers, Inc. 3 Park Avenue, New York, NY 10016-5997, USA (2002).
[16] Arrubla, J., Farrher, E., Strippelmann, J., Tse, D. H. Y., Grinberg, F., Shah, N. J., & Neuner, I., "Microstructural and functional correlates of glutamate concentration in the posterior cingulate cortex," Journal of Neuroscience Research, 95, no. 9, 1796-1808 (2017). doi:10.1002/jnr.24010
[17] Wu, X., Wu, T., Zhan, Z., Yao, L., & Wen, X., "A real-time method to reduce ballistocardiogram artifacts from EEG during fMRI based on optimal basis sets (OBS)," Computer Methods and Programs in Biomedicine, 127, 114-125 (2016). doi:10.1016/j.cmpb.2016.01.018
[18] Murias, M., Webb, S. J., Greenson, J., & Dawson, G., "Resting state cortical connectivity reflected in EEG coherence in individuals with autism," Biological Psychiatry, 62(3), 270-273 (2007). doi:10.1016/j.biopsych.2006.11.012
[19] Simon, D.M., Damiano, C.R., Woynaroski, T.G. et al. "Neural Correlates of Sensory Hyporesponsiveness in Toddlers at High Risk for Autism Spectrum Disorder," J Autism Dev Disord, 47, Issue 9, 2710–2722 (2017). doi:10.1007/s10803-017-3191-4
[20] Ala, G., Fasshauer, G., Francomano, E., Ganci, S., & McCourt, M., "The method of fundamental solutions in solving coupled boundary value problems for M/EEG," SIAM Journal on Scientific Computing, 37(4), B570-B590 (2015). doi:10.1137/13094921X
[21] Ala, G., Francomano, E., Fasshauer, G. E., Ganci, S., & McCourt, M. J., "A meshfree solver for the MEG forward problem," IEEE Transactions on Magnetics, 51(3), (2015). doi:10.1109/TMAG.2014.2356134